

Supporting Information

A dual-mode probe based on AIE and TICT effects for the detection of hypochlorite anion and its bioimaging in living cells

Yang Zhou, Hai Xu, Qing-Xiu Li, Zong-Rui Hou*, Ya-Wen Wang*, and Yu Peng

School of Life Science and Engineering, Southwest Jiaotong University,
Chengdu 610031, People's Republic of China

h zr@swjtu.edu.cn, ywwang@swjtu.edu.cn

Table of Contents

1. General Methods.....	2
2. Comparison of hypochlorite anion fluorescent probes.....	4
3. Synthesis of the M-CHO and SWJT-12	5
4. ¹ H NMR and ESI-MS copies of M-CHO	6
5. ¹ H NMR and MS copies of SWJT-12	8
6. Basic properties of SWJT-12	12
7. LC-MS spectrum of probe SWJT-12 and ClO ⁻	19
8. Energy distribution of SWJT-12 and MB	20
9. Cytotoxicity of SWJT-12 in living HeLa cells	22

1. General Methods.

Aniline, terephthalaldehyde, acetic acid, p-Anisil, ammonium acetate, 2,3-diaminodinitrile, ethanol, deionized water, ClO^- , Cys and other analytical reagents were all purchased from Innochem Technology Co., Ltd.

^1H and ^{13}C NMR spectra were recorded on a Bruker AVB-400 spectrometer using TMS as the internal reference. ESI-MS spectra were acquired on a Bruker Esquire 6000 spectrometer. HRMS spectra were acquired on a Bruker micrOTOF-Q III. LC-MS spectra were acquired on an Alliance HPLC E2695. Fluorescence spectra were recorded by a Hitachi F-7000 spectrophotometer. Fluorescence imaging of ClO^- in HeLa cells was recorded on a Nikon A1R+ (Japan) laser scanning confocal microscope.

The solution of **SWJT-12** (1 mM) was prepared separately in methanol for the detection of the selectivity of the probes as ratiometric probes. Stock solutions of various analytes such as ClO^- , Cys, K^+ , Na^+ , Zn^{2+} , Ca^{2+} , Mg^{2+} , Fe^{3+} , Cl^- , SO_4^{2-} , DTBP, H_2O_2 (1.0 mM) were obtained with PBS. All detection experiments in this study were performed at 37 °C in 10 mM PBS buffer- CH_3OH (98:2, v/v).

Portable test paper After preparing a methanol solution containing 10.0 μM **SWJT-12**, carefully place the filter paper strip in it and soak it well. Then the filter paper strip was taken out and vacuum-dried, and finally a portable test strip was successfully produced. Subsequently, after spraying with different concentrations of ClO^- , the changes in fluorescence were directly observed from the portable test strips under 365 nm UV light irradiation.

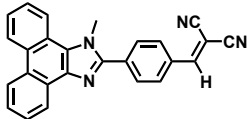
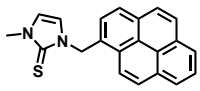
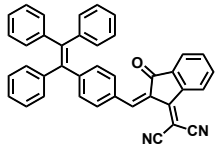
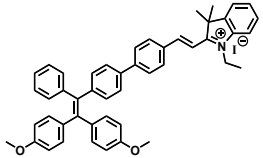
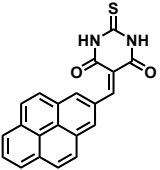
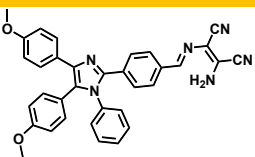
HeLa cells (human cervical cancer cells) were plated in 96-well plates and incubated in a 5% carbon dioxide, 37°C incubator for 24h. After removing the medium, add probes of different concentrations (0, 10.0 μM , 25.0 μM , 50.0 μM) to the fresh medium for 24 hours in an incubator. Then, 10.0 μL of MTT (5 mg/mL in PBS, pH 7.4) was added to each well, and after the cells were incubated for another 2 hours, the culture supernatant was removed, and the resulting formazan crystals were dissolved in 150 μL of dimethyl sulfoxide. Next, the plates were incubated for an additional 10 minutes at 37°C on a shaker at 60-70 rpm. Finally, the absorbance (A)

of each well at 570 nm was measured using a microplate reader. (Cell relative viability = $A_{\text{sample}} / A_{\text{control}} * 100\%$).

HeLa cells were plated in glass bottom dishes with fresh medium and incubated in a 37°C incubator for 24 hours. After washing with PBS buffer, fresh medium and 25.0 μM probe were added and incubated for 1 h. After washing three times with PBS buffer, the medium and 150.0 μM ClO^- were added for treatment for 30 min. Finally, after washing three times with PBS buffer, the dishes were placed on a confocal laser scanning microscope for cell imaging.

2. Comparison of hypochlorite anion fluorescent probes.

Table S1. The comparison of the reported ClO⁻ fluorescent probes.

Probe	AIE based	Solution	Fluorescence change	Theoretical calculation support	Application of portable test strips	Ref.
	-	DMSO/PBS (50:50, v/v)	Ratiometric	✓	-	[10a]
	-	DMF/PBS (5:95, v/v)	Ratiometric	-	-	[10b]
	✓	THF/H ₂ O (1: 4, v/v)	Ratiometric	✓	-	[10c]
	✓	CH ₃ OH/PBS (1:9 v/v)	Turn-on	✓	✓	[10d]
	✓	DMSO/H ₂ O (5:95, v/v)	Turn-on	✓	-	[10e]
	✓	CH ₃ OH/PBS (2:98, v/v)	Ratiometric	✓	✓	<i>This Work</i>

3. Synthesis of the **M-CHO** and **SWJT-12**.

M-CHO was synthesized according to literature reports.¹² Aniline (93 mg, 1.0 mmol) and terephthalaldehyde (134 mg, 1.0 mmol) were dissolved in acetic acid (15 mL) and reacted at room temperature. After 1 h, *p*-Anisil (270 mg, 1.0 mmol) and ammonium acetate (539 mg, 7.0 mmol) were added to the reaction flask to react at 120 °C for 10 h to obtain **M-CHO**. ¹H NMR (400 MHz, CDCl₃): δ 9.96(s, 1H), 7.75-7.72(m, 2H), 7.61-7.58(m, 2H), 7.55-7.51(m, 2H), 7.34-7.28(m, 3H), 7.08-7.02(m, 4H), 6.84-6.80(m, 2H), 6.78-6.75(m, 2H), 3.79-3.77(d, *J* = 7.0 Hz, 6H) ppm. ESI-MS: *m/z* 461.3 [M+H]⁺.

The synthetic procedures of **SWJT-12** were shown in Scheme 1. **M-CHO** (46 mg, 0.1 mmol) and 2,3-diaminodinitrile (12 mg, 0.12 mmol) were dissolved in absolute ethanol (8 mL), and 1 drop of concentrated sulfuric acid was added. Then, the solution was stirred at 78 °C for 30 min. After cooling to room temperature, the precipitate was filtered, washed with absolute ethanol, and then washed with distilled water to obtain **SWJT-12** as a yellow powder with a yield of 85%. ¹H NMR (400 MHz, CDCl₃): δ 8.29 (s, 1H), 7.66–7.64 (d, *J* = 8.1 Hz, 2H), 7.53–7.48 (t, *J* = 9.2 Hz, 4H), 7.35–7.26 (q, *J* = 6.6 Hz, 3H), 7.08–7.03 (dd, *J* = 13.5, 7.4 Hz, 4H), 6.83–6.75 (dd, *J* = 23.3, 8.3 Hz, 4H), 5.57 (s, 2H), 3.78–3.77 (d, *J* = 6.7 Hz, 6H) ppm. ¹³C NMR (100 MHz, CDCl₃) δ 159.35, 158.61, 157.71, 138.65, 137.06, 134.22, 134.06, 132.35, 129.32, 129.00, 128.82, 128.60, 128.53, 128.42, 126.91, 124.99, 122.40, 113.93, 113.74, 107.72, 77.36, 77.04, 76.73, 55.22, 55.15 ppm. ESI-MS: *m/z* 551.3 [M+H]⁺. HRMS (ESI): calcd for C₃₄H₂₇N₆O₂ [M+H]⁺ 551.2190, found 551.2192.

4. ^1H NMR and ESI-MS copies of M-CHO.

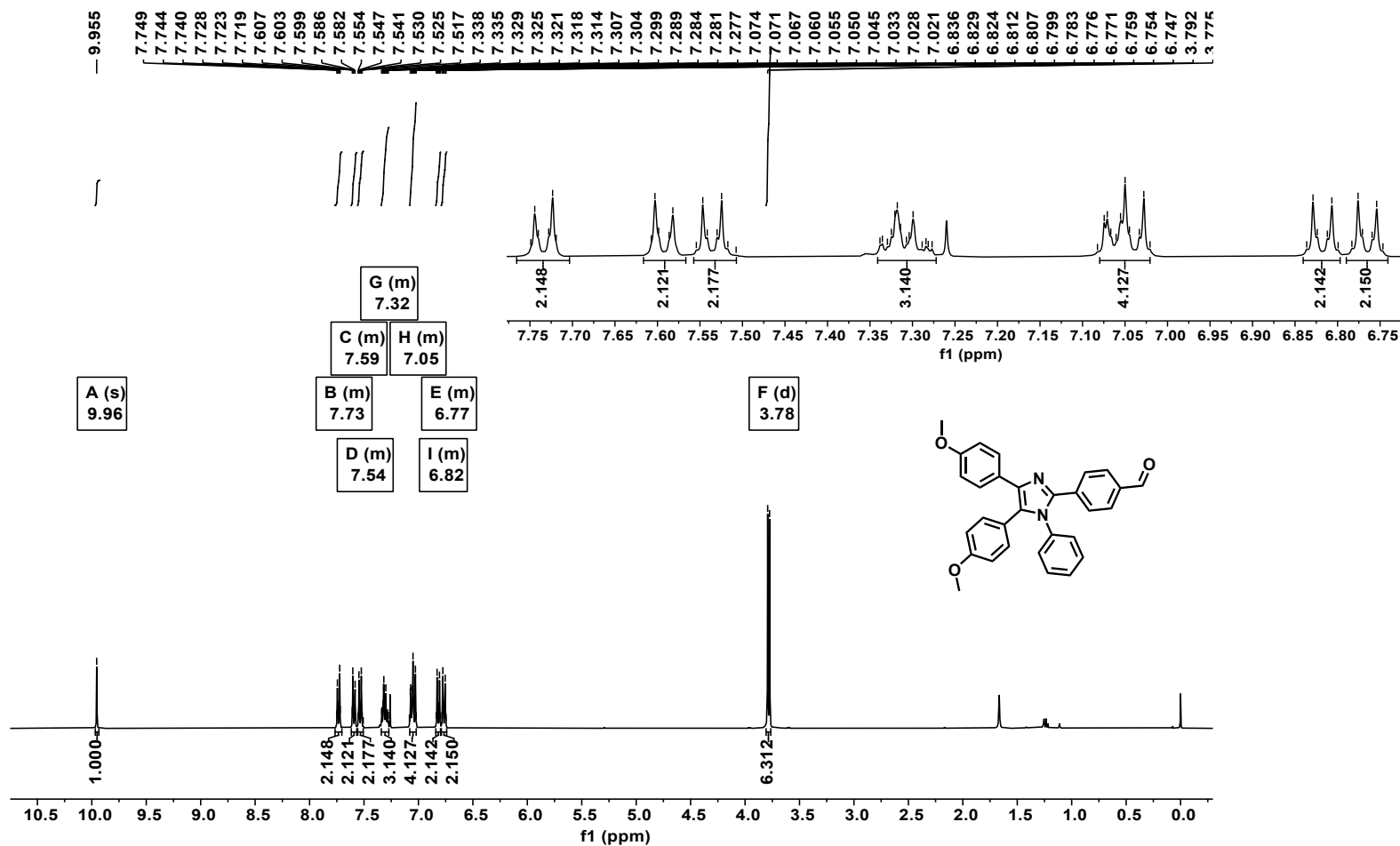


Figure S1. ^1H NMR spectrum of probe M-CHO (400 MHz, CDCl_3).

Generic Display Report

Analysis Info
Analysis Name D:\Data\yangy\newWANGBAOJUN20220512_1_21_01_45694.d Acquisition Date 5/12/2022 12:51:05 PM
Method POS_100-1200_For LC.m Operator LZU
Sample Name WANGBAOJUN20220512_1 Instrument micrOTOF
Comment

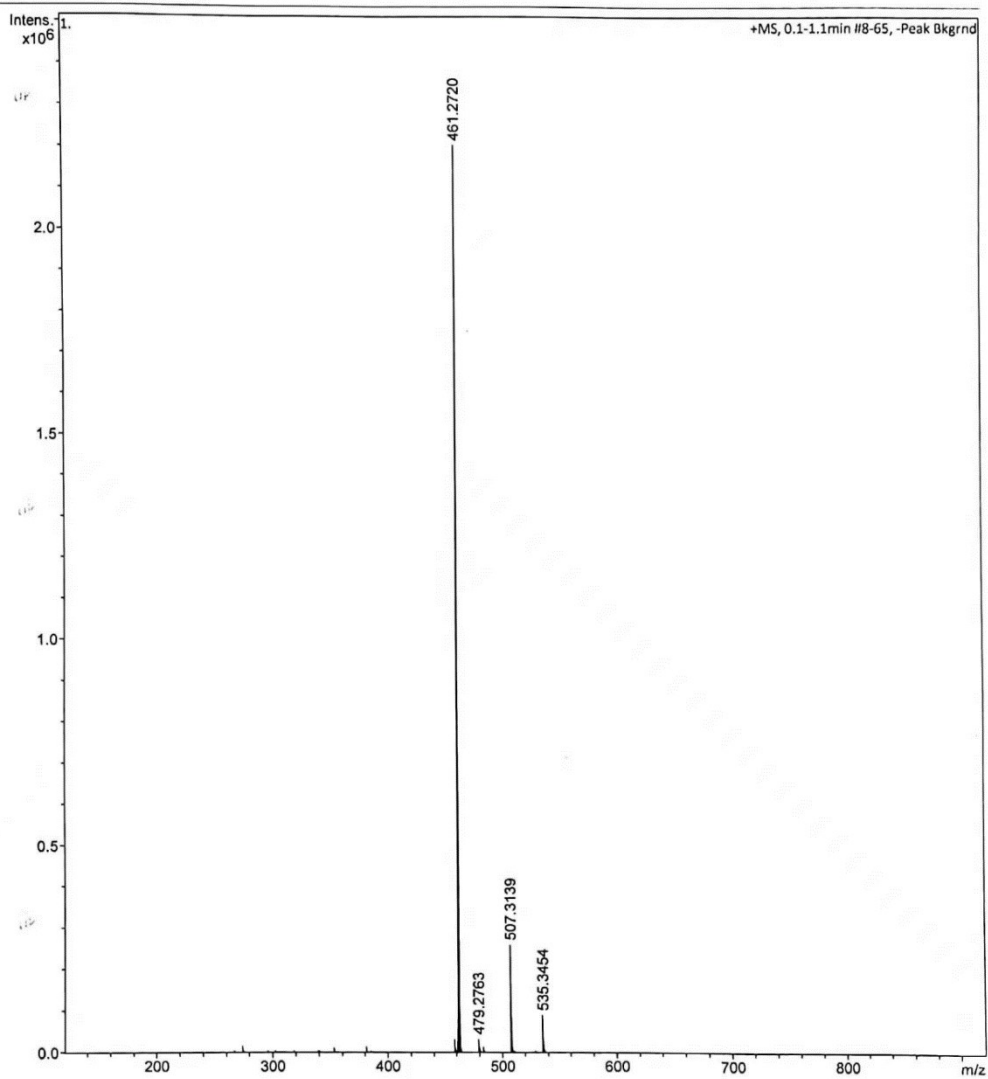


Figure S2. ESI-MS spectrum of M-CHO.

5. NMR and MS copies of SWJT-12.

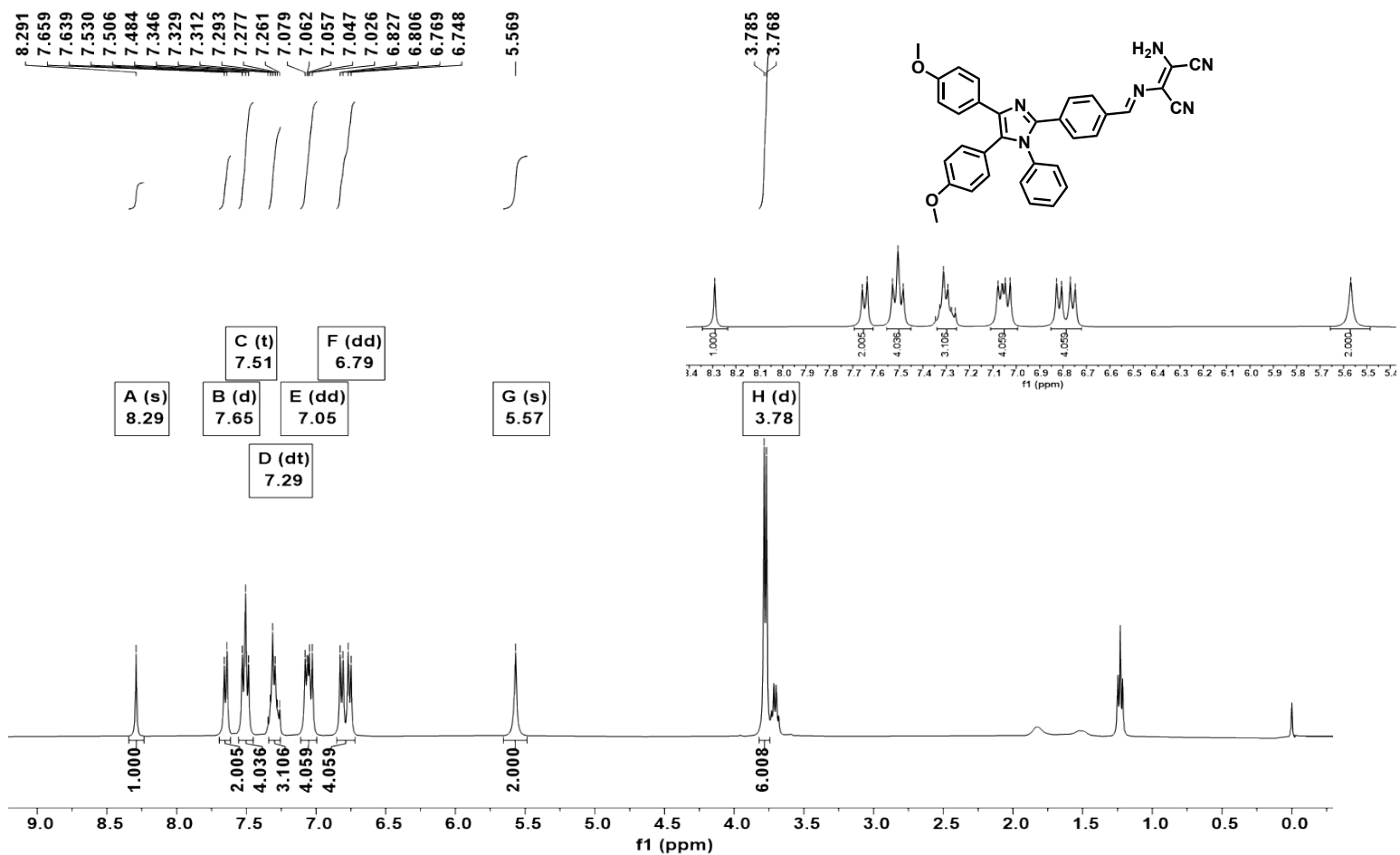


Figure S3. ^1H NMR spectrum of probe SWJT-12 (400 MHz, CDCl_3).

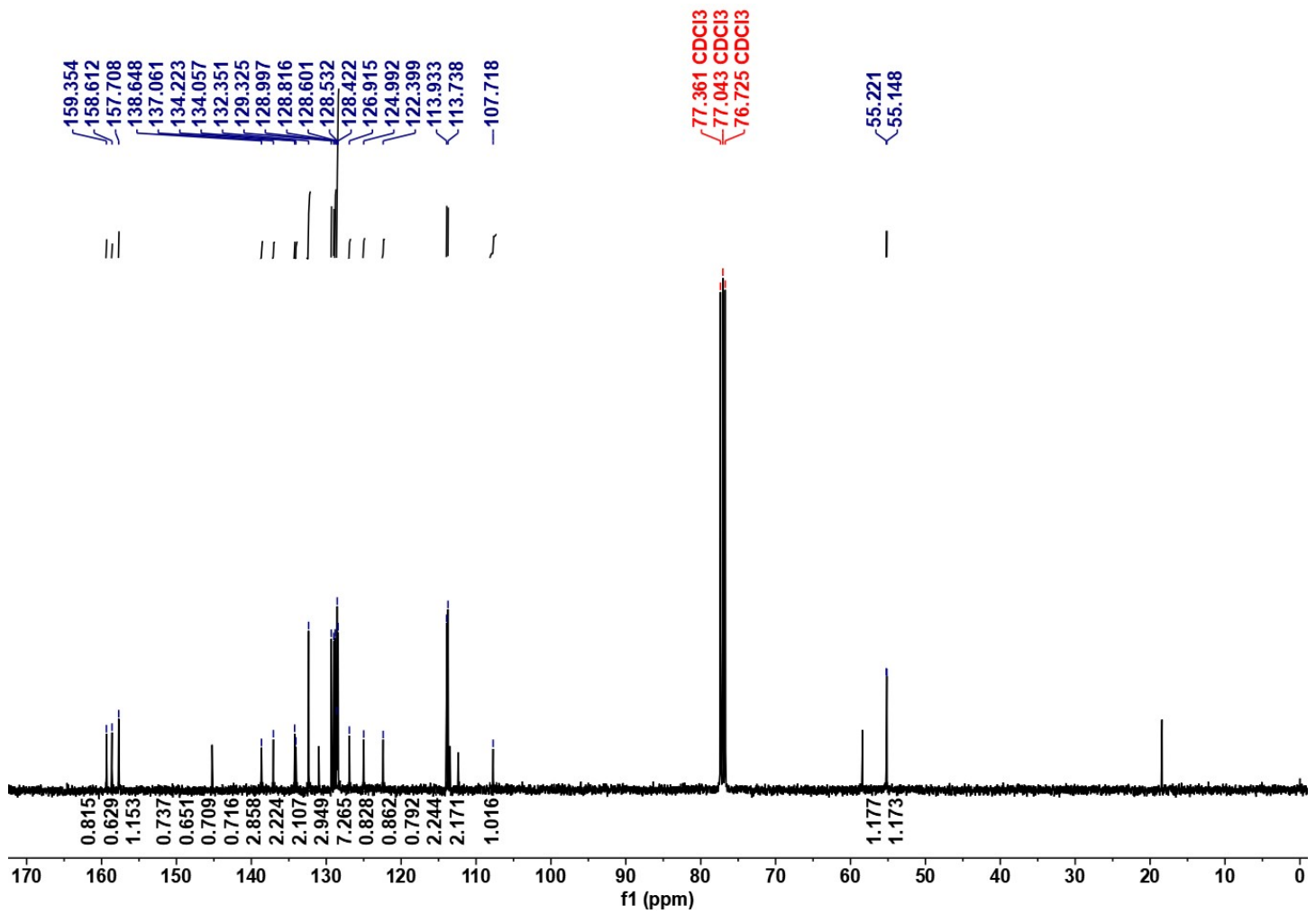


Figure S4. ^{13}C NMR spectrum of probe SWJT-12 (100 MHz, CDCl_3).

Generic Display Report

Analysis Info		Acquisition Date	5/12/2022 12:54:12 PM
Analysis Name	D:\Data\yangy\new\WANGBAOJUN20220512_2_22_01_45695.d	Operator	LZU
Method	POS_100-1200_For LC.m	Instrument	micrOTOF
Sample Name	WANGBAOJUN20220512_2		
Comment			

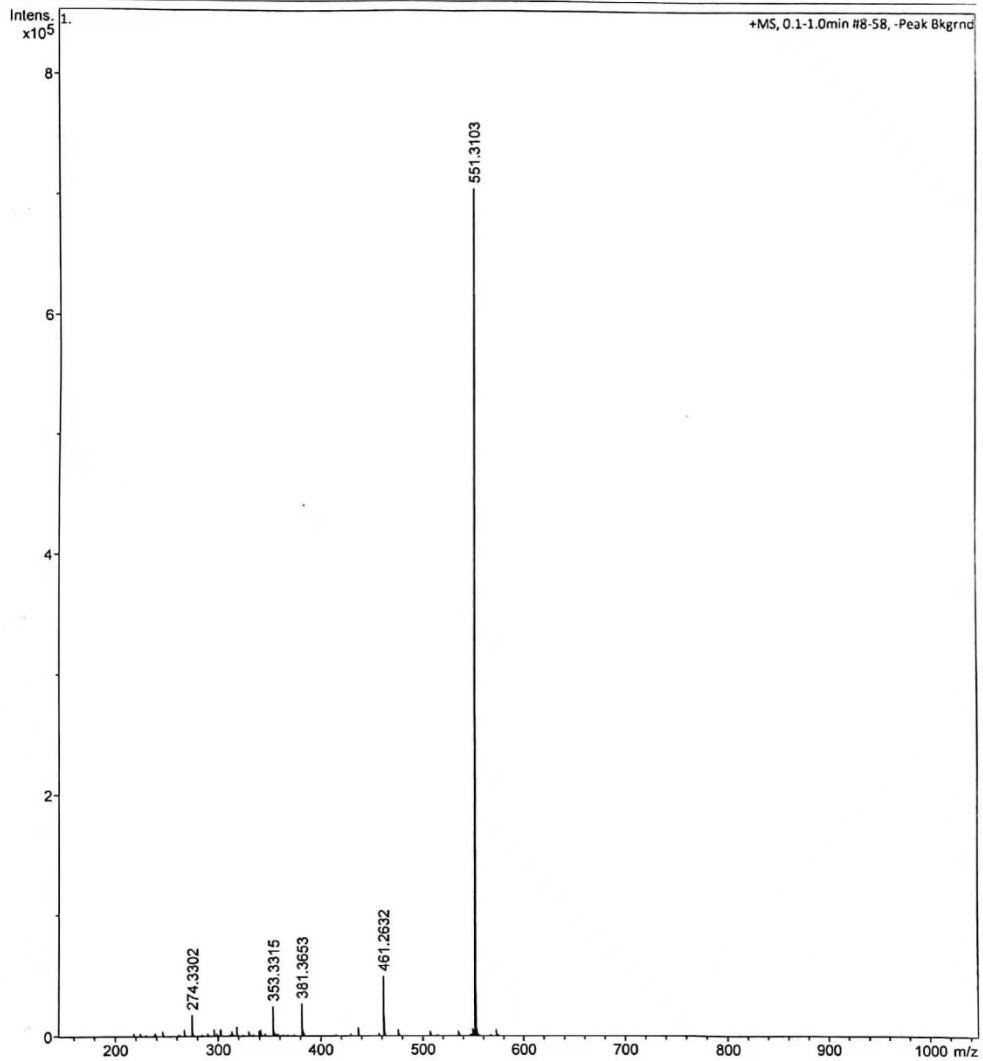


Figure S5. ESI-MS spectrum of probe SWJT-12.

Display Report

Analysis Info
Analysis Name: D:\Data\220630\S-1209-2_RA1_01_868.d
Method: LCMS.m
Sample Name: S-1209-2
Comment:
Acquisition Date: 12/9/2022 4:55:44 PM
Operator: BDAL@DE
Instrument: micrOTOF-Q III 8228888.20485

Acquisition Parameter

Source Type	ESI	Ion Polarity	Positive	Set Nebulizer	2.0 Bar
Focus	Active	Set Capillary	3000 V	Set Dry Heater	200 °C
Scan Begin	50 m/z	Set End Plate Offset	-500 V	Set Dry Gas	8.0 l/min
Scan End	1000 m/z	Set Collision Cell RF	140.0 Vpp	Set Divert Valve	Waste

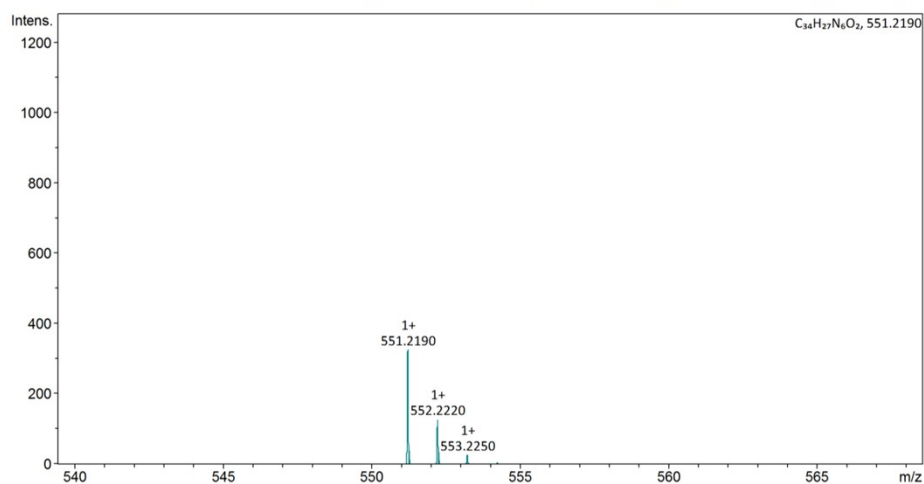
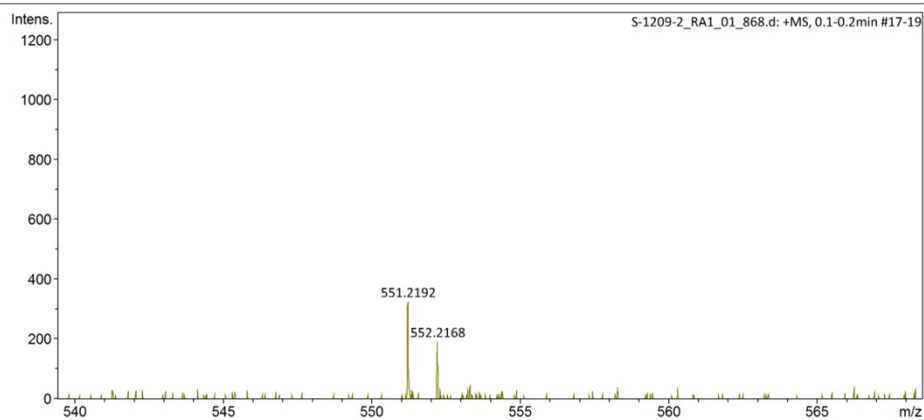


Figure S6. HRMS spectrum of probe SWJT-12

6. Basic properties of SWJT-12.

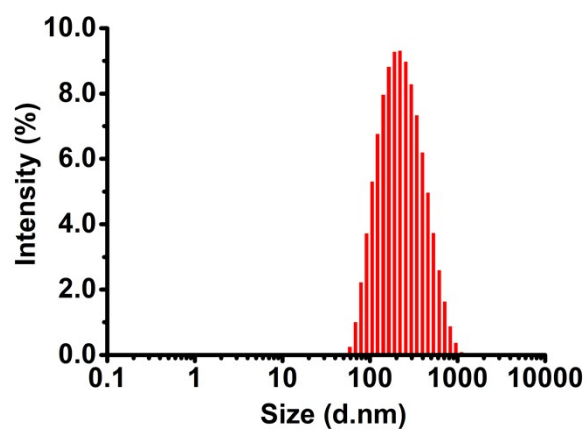


Figure S7. Size distribution of SWJT-12 in the aggregated state in 98% PBS buffer solution (pH = 7.4).

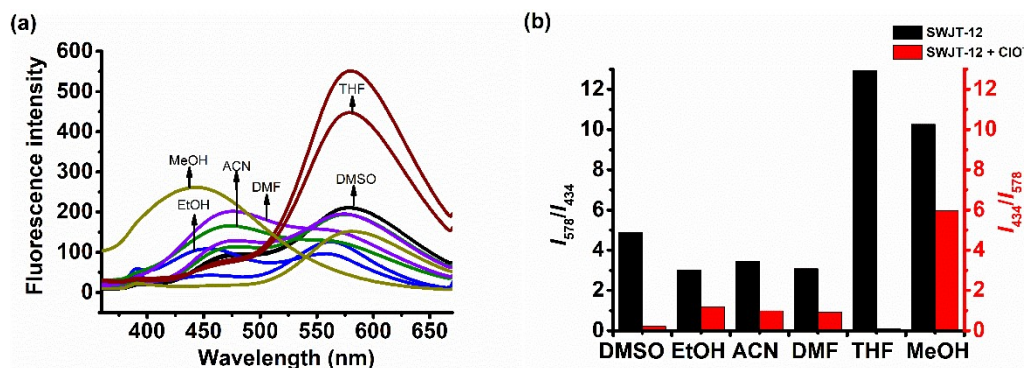


Figure S8. Fluorescence spectra of SWJT-12 in different solvents in the absence and presence of ClO^- ($90.0 \mu\text{M}$) in 98% PBS buffer solution ($\text{pH} = 7.4$) ($\lambda_{\text{ex}} = 340 \text{ nm}$).

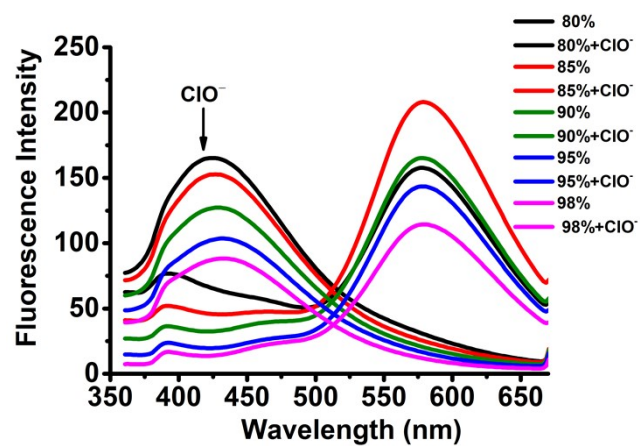


Figure S9. Fluorescence intensity versus the content of the CH₃OH/PBS mixture of SWJT-12 in the presence of ClO⁻ (90.0 μM) ($\lambda_{\text{ex}} = 340$ nm).

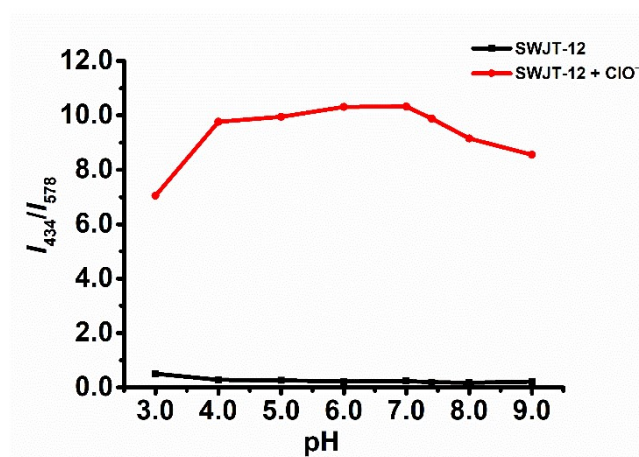


Figure S10. Fluorescence responses of SWJT-12 and SWJT-12 + ClO⁻ (90.0 μ M) in PBS buffer solution (2% CH₃OH) under different pH conditions ($\lambda_{\text{ex}} = 340$ nm).

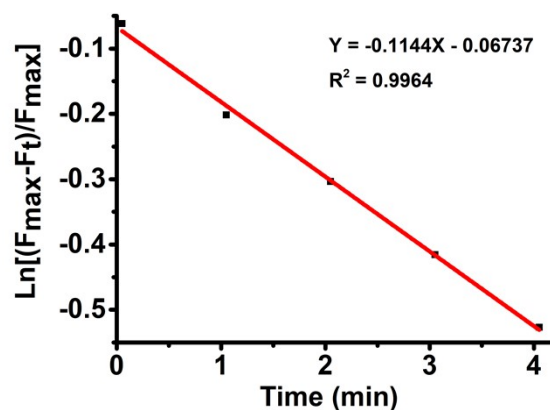


Figure S11. Pseudo first-order kinetic plots of **SWJT-12** (10.0 μM) with the addition of ClO^- in PBS buffer solution (2% CH_3OH , $\text{pH} = 7.4$) ($\lambda_{\text{ex}} = 340 \text{ nm}$).

The result of the analysis as follows:

$$\ln [(F_{\text{max}} - F_t) / (F_{\text{max}})] = -k_{\text{obs}}t$$

$$t_{1/2} = \ln 2 / k_{\text{obs}}$$

Where F_{max} and F_t are the fluorescent intensity at maximum emission wavelength, and time t . k_{obs} is the pseudo-first-order rate constant.

$$k_{\text{obs}} = 1.91 \times 10^{-3} \text{ s}^{-1}$$

$$t_{1/2} = 6.06 \text{ min}$$

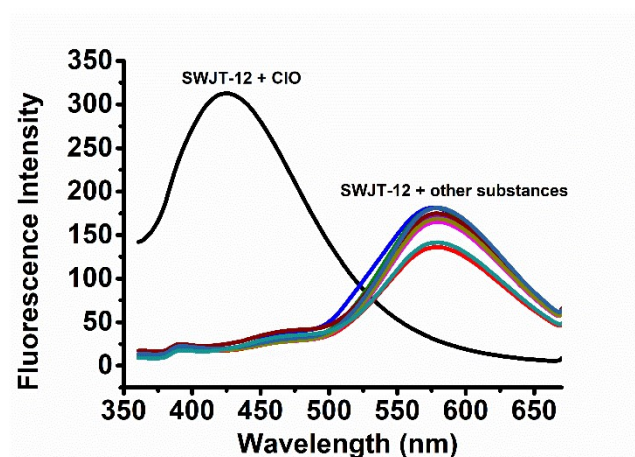


Figure S12. Selectivity studies of SWJT-12 (10.0 μM) for different kinds of analytes (90.0 μM) ($\lambda_{\text{ex}} = 340 \text{ nm}$).

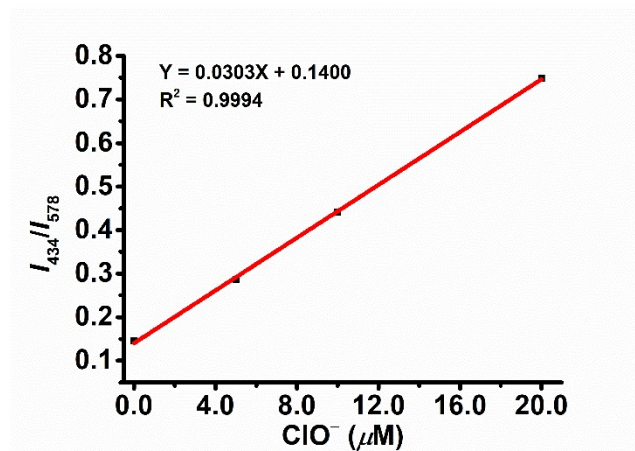


Figure S13. Linear relationship between the ratio of fluorescence at 434 nm and 578 nm and ClO⁻ concentration from 0.0 to 20.0 μM in PBS buffer solution (2% CH₃OH, pH = 7.4) (λ_{ex} = 340 nm).

The below equation was used for the plot that determined the LOD.

The result of the analysis as follows:

$$\text{Linear Equation: } Y = 0.0303 \times X + 0.1400$$

$$\delta = \sqrt{\frac{\sum (F_0 - \bar{F}_0)^2}{N - 1}} = 0.0028 \text{ (N = 10); } \quad S = 0.0303; \quad K=3;$$

$$\text{LOD} = K \times \delta / S = 0.28 \mu\text{M}$$

7. LC-MS spectrum of probe SWJT-12 and ClO⁻.

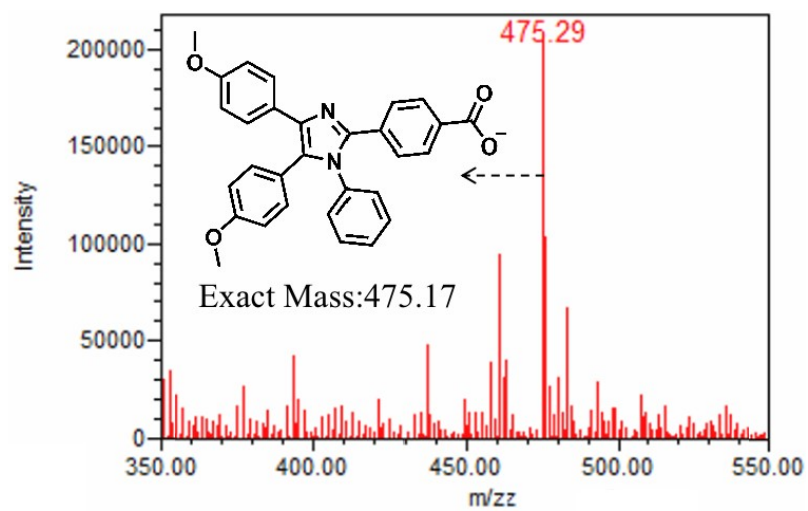


Figure S14. LC-MS profiles of SWJT-12 and ClO⁻ (1.0 equiv).

8. Energy distribution of SWJT-12 and MB.

No.	Energy (cm ⁻¹)	Wavelength (nm)	Osc. Strength	Symmetry	Major contribs	Minor contribs
1	19348.56784	516.834118	0.4325	Singlet-A	HOMO->LUMO (99%)	
2	26042.20928	383.992	0.6674	Singlet-A	H-2->LUMO (12%), H-1->LUMO (84%)	
3	27656.9424	361.57287	0.3115	Singlet-A	H-2->LUMO (71%), HOMO->L+1 (21%)	H-1->LUMO (6%)
4	28981.31392	345.04992	0.0651	Singlet-A	H-2->LUMO (13%), HOMO->L+1 (62%)	H-4->LUMO (5%), H-3->LUMO (5%), H-1->LUMO (6%), HOMO->L+2 (6%), HOMO->L+3 (3%)
5	30336.33472	329.63771	0.0242	Singlet-A	HOMO->L+2 (85%)	H-4->LUMO (4%), H-3->LUMO (4%), HOMO->L+1 (3%)
6	30729.936	325.41558	0.015	Singlet-A	H-3->LUMO (11%), HOMO->L+3 (82%)	HOMO->L+2 (4%)
7	31046.91408	322.0932	0.0109	Singlet-A	H-3->LUMO (75%), HOMO->L+3 (10%)	H-4->LUMO (8%), HOMO->L+1 (4%)
8	31659.09312	315.86502	0.0178	Singlet-A	H-4->LUMO (73%), H-1->L+1 (11%)	HOMO->L+1 (7%), HOMO->L+2 (2%), HOMO->L+3 (2%)
9	32625.352	306.5101	0.0006	Singlet-A	H-6->LUMO (37%), H-5->LUMO (46%)	HOMO->L+6 (7%)
10	33238.3376	300.85741	0.0024	Singlet-A	H-7->LUMO (19%), H-6->LUMO (21%), H-5->LUMO (38%)	HOMO->L+4 (9%), HOMO->L+5 (5%), HOMO->L+6 (4%)

Figure S15. Energy distribution of SWJT-12.

No.	Energy (cm ⁻¹)	Wavelength (nm)	Osc. Strength	Symmetry	Major contribs	Minor contribs
1	25770.39856	388.0421165	0.3159	Singlet-A	HOMO->LUMO (99%)	
2	30642.82752	326.3406418	0.0347	Singlet-A	HOMO->L+1 (90%)	HOMO->L+2 (7%)
3	31235.64912	320.1470205	0.0192	Singlet-A	HOMO->L+2 (91%)	HOMO->L+1 (7%)
4	32922.97264	303.7392798	0.1872	Singlet-A	H-1->LUMO (97%)	
5	33515.79424	298.3667917	0.0697	Singlet-A	HOMO->L+3 (75%), HOMO->L+4 (22%)	
6	34203.78992	292.365262	0.1534	Singlet-A	HOMO->L+3 (21%), HOMO->L+4 (74%)	
7	35794.32624	279.3738855	0.0168	Singlet-A	H-5->LUMO (10%), HOMO->L+5 (74%)	H-4->LUMO (7%), H-2->LUMO (4%)
8	36124.20928	276.8226682	0.3004	Singlet-A	H-2->LUMO (89%)	HOMO->L+5 (3%), HOMO->L+7 (2%)
9	37384.056	267.4937144	0.0405	Singlet-A	H-3->LUMO (84%)	H-8->LUMO (3%), H-6->LUMO (2%), H-4->LUMO (6%)
10	37602.63376	265.9388186	0.0112	Singlet-A	HOMO->L+6 (78%)	H-3->L+3 (4%), H-3->L+7 (3%), HOMO->L+7 (8%)

Figure S16. Energy distribution of **MB**.

9. Cytotoxicity of SWJT-12 in living HeLa cells.

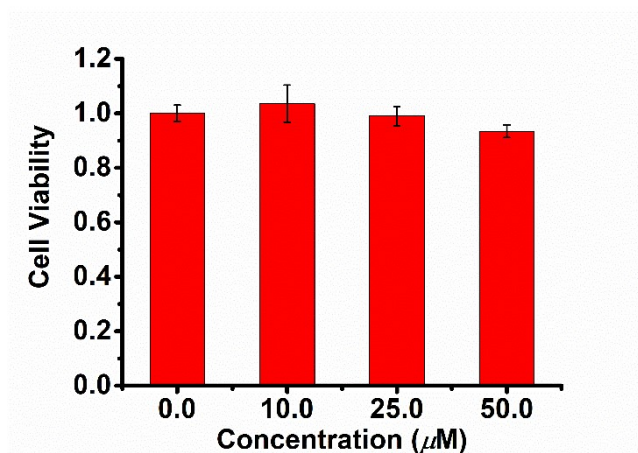


Figure S17. The viability of HeLa cells was determined by MTT assay after incubation with different concentrations of **SWJT-12** for 24 h.